ISSN 2564-3258

CASE REPORT

Unusual Presentation of Erdheim-Chester Disease Complicated by Severe Hypercalcemia in a 25-Year-Old Male: Initial Assessment and Follow-up with ^{18} F-fluorodeoxyglucose-Positron Emission Tomography and 3 Tesla MR Imaging

Joshua Everhart[1], O Hans Iwenofu[2], Joseph S Yu*[3]

Everhart J, Iwenofu O H, Yu J S. Unusual Presentation of Erdheim-Chester Disease Complicated by Severe Hypercalcemia in a 25-Year-Old Male: Initial Assessment and Follow-up with ^{18} F-fluorodeoxyglucose-Positron Emission Tomography and 3 Tesla MR Imaging. Int J Radiol Case Rep. 2021;1(1):01-09.

Abstract

We present a newly diagnosed case of Erdheim-Chester disease in a patient who presented with influenza-like symptoms, and whose course was complicated with life-threatening hypercalcemia. The imaging features were characteristic, and diagnosis was confirmed with immunohistochemical staining. The FDG-PET-CT was useful in diagnosis and follow-up.

Key Words: *Erdheim-Chester; Histiocytosis; PET-CT; Osteosclerosis; Hypercalcemia*

Introduction

Erdheim-Chester disease (ECD) is a rare, systemic non-Langerhans cell histiocytosis of unknown etiology. Since its initial description by Jakob Erdheim and William Chester in 1930, about 500 to 550 cases have been reported [1,2]. Nearly all patients have osseous involvement, characteristically affecting the appendicular skeleton, and nearly 60% show variable extraosseous involvement, particularly of the heart and nervous system [3,4]. A classic triad of diabetes insipidus, bone pain, and bilateral exophthalmos is nearly diagnostic of ECD [5].

The radiographic feature of symmetric diaphyseal and metaphyseal osteosclerosis with loss of the corticomedullary differentiation is characteristic of ECD [5-7]. The appearance of ECD on ^{99}Technetium bone scintigraphy is abnormal uptake in the metadiaphyseal regions of the long bones that typically corresponds with the radiographic abnormalities but occasionally it may reveal an affected area that is radiographically normal [3,6]. The appearance of ECD on magnetic resonance (MR) imaging is homogeneously low signal intensity in the marrow and heterogeneously increased signal intensity on fluid sensitive sequences along the diaphysis and metaphysis with variable involvement the epiphysis

[1]*Department of Orthopedic Surgery, Indiana University, 550 N. University Blvd, Indianapolis, IN, 46202*

[2]*Department of Pathology, The Ohio State University Wexner Medical Center, 1645 Neil Avenue, Columbus, OH 43210*

[3]*Department of Radiology, The Ohio State University Wexner Medical Center, 395 West 12th Avenue, Columbus, OH 43210*

[*]*Corresponding author: Joseph S Yu, M.D., Professor of Radiology and Orthopedic Surgery, Director of Musculoskeletal Imaging, The Ohio State University Medical Center, 395 West 12th Avenue, Suite 481 Columbus, OH 43210, USA, Tel: (614) 293-8315; Fax: (614) 293-6935; E-mail: Joseph.yu@osumc.edu*

Received: February 19, 2021, Accepted: April 18, 2021, Published: July 31, 2021

[3,7-9]. ^{18}F-labeled fluorodeoxyglucose (FDG) and 68Ga-DOTA-fibroblast activation protein (FAP) positron emission tomography PET/CT have been useful for detection of the primary lesion and for evaluating disease extent [10-15]. The specificity FDG-PET may be best served in differentiating ECD from other histiocytosis and for evaluating patients during follow-up of the disease [12,16].

We recently encountered a patient with newly diagnosed ECD whose hospital course was complicated by severe hypercalcemia after he was treated for an upper respiratory infection. Initial FDG-PET-CT scan showed FDG uptake in the long bones with an SUV_{max} ranging from 7.3 to 7.4, corresponding to avid areas in a 99mTechnetium bone scan. The transient hypercalcemic episode was likely produced by acute osseous inflammation that resulted in transient bone lysis manifested as marrow signal changes and intense periostitis on a 3 Tesla MR imaging scan. Aggressive treatment of the hypercalcemia resulted in eventual normalization of the serum calcium and marked improvement of the FDG uptake in the skeleton on a follow-up FDG-PET-CT scan that was performed 12 weeks later even though the ECD itself had not been treated.

Case Report

A 25-year-old white male presented to the emergency department (ED) with influenza-like symptoms for one-week and episodic febrile episodes to 104°F. He was diagnosed with a bacterial pharyngitis and was given one dose of intramuscular ceftriaxone. While in the ED, he developed an ascending rash and chest tightness and was subsequently treated for a drug reaction with antihistamines and eventually discharged. In the following days, the febrile episodes persisted and he developed ataxia and pain in both lower extremities.

On admission, his temperature was measured at 103°F and he was tachycardic. In addition to increasing pain in his lower extremities, he also endorsed new-onset arthralgias in the ankle, knee and hip joints and painful upper extremities. Positive findings on physical examination included diffuse edema in the calves, and generalized warmth and tenderness in both lower extremities. Similar but less pronounced findings were present in the upper extremities affecting the upper arms and shoulders. Cervical adenopathy was noted. No ocular or cutaneous lesion was observed. Laboratory tests performed on admission revealed an increased erythrocyte sedimentation rate (60 mm/h, normal 0-14 mm/h) and C-reactive protein (319 mg/dL, normal 0-9.99 mg/dL). There was generalized pancytopenia (WBC 3.3 K/mL, RBC 3.3 M/mL, hemoglobin 9.8 g/dL, and hematocrit 28.5%). Electrolyte and calcium levels were normal. His past medical history was significant only for progressively worsening dentition with painless gingivitis and loosening of the teeth which was confirmed on inspection. There was no prior history of cardiovascular disease, ocular disease including exophthalmos, endocrine abnormalities, cutaneous pathology, renal disease, pulmonary disease, or neurological disorders.

Several imaging studies were performed on admission. A chest radiograph showed lower lobe infiltrates. Computed tomography (CT) of the chest showed bilateral pleural effusions in addition to bibasilar consolidations but no evidence of interstitial disease. The aorta and the heart appeared normal. Mild enlargement of cervical lymph nodes was noted. An abdominal and pelvis CT showed mild splenomegaly but the kidneys appeared normal. There was no evidence of retroperitoneal fibrosis. A lytic lesion was identified in the left ilium as well as in the L2 vertebra. Both proximal femora and lower extremities (Figure 1) showed diffuse heterogeneous osteosclerosis and loss of the corticomedullary junction. There were similar findings in the upper extremity. Follow-up CT of the pelvis (Figure 2) showed sclerotic changes in both proximal femora and areas of diminished attenuation in both femoral necks.

Figure 1) *Radiographs of the pelvis (a), lateral proximal left femur (b), and frontal proximal right tibia and fibula show diffusely increased bone density throughout the appendicular long bones with loss of the corticomedullary junction.There is region of decreased density in the left femoral neck (arrows).*

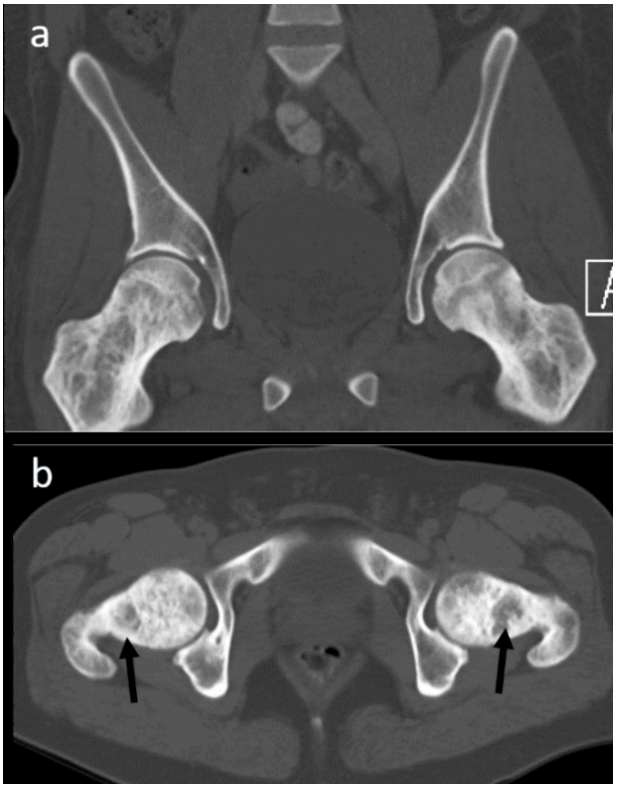

Figure 2) *Pelvis CT without contrast. Bilateral diffuse sclerotic lesions with lytic components (arrows) are evident in the proximal femora corresponding to the radiographic findings.*

In the next two of days of hospitalization, a ^{99m}Technetium bone scan and 18F FDG PET-CT scan was performed to search for a neoplastic process. The bone scan showed diffusely increased radionuclide uptake in the meta-diaphyseal regions of the long bones, and about the knee, hip, and shoulder regions (Figure 3). The 18F FDG PET-CT scan showed diffuse hypermetabolic activity in the same distribution as the bone scan with focal intense areas of FDG uptake within the proximal femora (SUV_{max} was 7.3 in left femur, 7.4 in right femur), knee and both humeri, and intense activity in the maxillary sinuses related to sinusitis (Figure 4). An MR examination of the hip joints and proximal femora was performed to further characterize the PET-CT scan findings and regions of osteosclerosis. On T1-weighted images, low signal intensity was noted throughout both femora which appeared much more heterogeneous than previously reported in the literature. On the fat-saturated T2-weighted images, the marrow demonstrated more pronounced heterogeneity with multiple focal areas of relatively hyperintense signal with larger foci corresponding to FDG-avid areas. Additionally, intense diffuse periostitis was noted bilaterally extending from the proximal metaphysis to the distal metaphysis. The hyperintense medullary lesions and periostitis enhanced with administration of intravenous gadolinium (Figure 5).

Figure 3) *(a) ^{99m}Technetium bone scintigraphy scan demonstrates multifocal increased radiotracer uptake with symmetric appearance involving the long bones of the arms and legs in addition to the maxilla. (b and c) ^{18}F-FDG PET-CT overlay. Diffuse hypermetabolic lesions (arrows) are noted throughout the axial and appendicular skeleton that are most intense in the proximal femurs and the maxilla. Hypermetabolic activity in the bilateral maxillary sinuses, tonsils, and cervical lymph nodes is suggestive of an infectious or inflammatory process.*

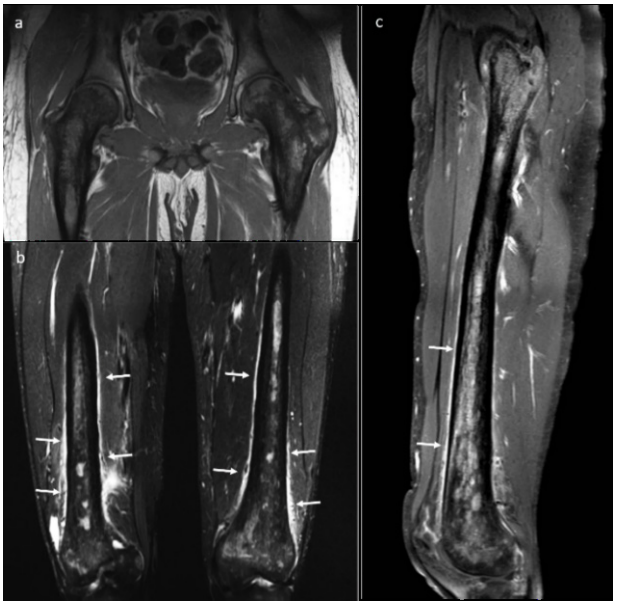

Figure 4) *(a) Coronal T1-weighted magnetic resonance image of the pelvis and proximal femora shows heterogeneously low signal intensity bone marrow. (b) Coronal short inversion-recovery image shows focal scattered regions of marrow hyperintensity and diffuse periosteal reactive changes in the metadiaphysis of both femora (arrows). (c) Sagittal fat-saturated T1-weighted image after administration of intravenous gadolinium shows enhancement of the marrow and the periosteum (arrows).*

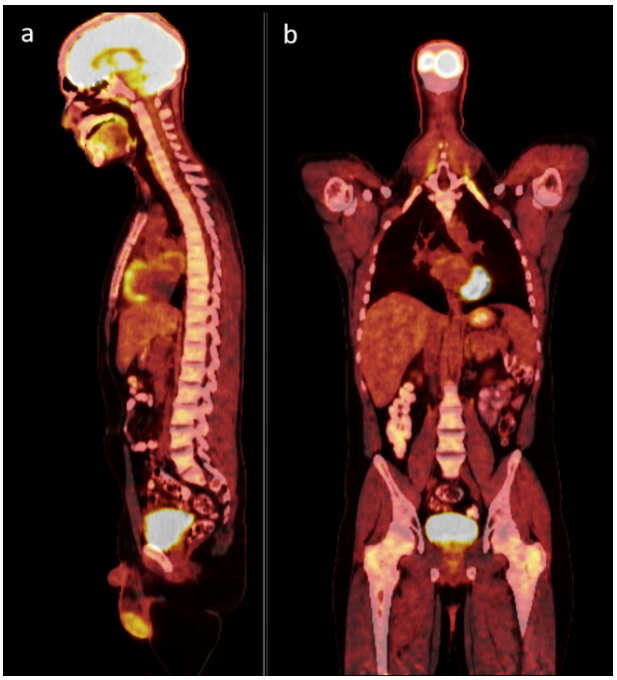

Figure 5) *Follow-up ^{18}F-FDG PET-CT of skull base to mid-thigh approximately 12 weeks after the episode of hypercalcemia. There was an interval decrease in SUV noted in the both proximal femora in areas of persistent diffuse osteosclerosis, and in the maxilla.*

Throughout the patient's hospitalization, repeated blood cultures were negative and an extensive battery of laboratory tests failed to identify evidence of a specific rheumatologic or autoimmune disorder eliminating the consideration of Still's disease which clinically was on the differential diagnosis. On the 6th hospital day, a biopsy of the affected region of the right proximal humerus was performed to determine if this was neoplastic. The pathology showed a granulomatous process with fibrotic cellular infiltrates composed predominantly of epithelioid histiocytes, plasma cells, and a lymphocytic inflammatory response. Immunohistochemical staining showed mixed T-and B-lymphocytes with positivity to CD3 and CD20 that indicated a predominant T-cell population. The histiocytic infiltrates were CD163 positive, CD207 (langerin) negative, and S-100 negative which was diagnostic for ECD. Additional imaging showed no evidence of extra-skeletal involvement. An echocardiogram and an unenhanced/enhanced MR scan of the brain were both normal. The hypothalamic-pituitary axis was normal based on clinical and laboratory findings.

On the 8th day of hospitalization, his calcium level began to increase and continued to escalate over the next 4 days, ultimately reaching a serum level of 13.4 mg/dL. At this point, the hypercalcemia had become severe and life-threatening, and treatment with aggressive hydration and administration of calcitonin was initiated with vigilant monitoring of his cardiac status. Sequential serum calcium levels after this episode showed a progressive decrease to normal subsequently requiring no additional treatment. At the time of discharge one week later, his febrile episodes had abated and the patient's skeletal symptoms had nearly resolved. Because of the rapid improvement in symptoms, the clinical service decided to postpone definitive therapy of his ECD with alpha-interferon (IFN-α) therapy until they had the results of his follow-up FDG PET-CT scan that was scheduled for 12 weeks after his discharge date. The follow-up PET-CT scan demonstrated a significant decrease in the SUV_{max} activity in the long bones (3.4 to 3.9) even without treatment (Figure 5). No further exacerbations have occurred and he has not yet begun treatment with IFN-α.

Discussion

Diagnosis of ECD is based on histologic findings of xanthomatous or xanthogranulomatous tissue infiltration by spumous histiocytes, 'lipid-laden' macrophages or histiocytes that are surrounded by fibrosis, with positivity to CD68 and CD163, and negativity to CD1a while S-100 immunohistochemical staining is generally negative [17-19]. The BRAF V600E mutation is prevalent in 38% to 100% of patients [1,17]. The contemporary classification of the World Health Organization arranges histiocytic disorders according to the type of histiocyte involved (dendritic cell disorders, macrophage-related disorders, and malignant histiocytic disorders) and ECD is classified as a dendritic disorder [20].

The mean age at diagnosis of ECD is approximately 55 years and there is a male predominance [21,22]. The 5-year survival rate of ECD was initially reported as 41% but recent reports indicate increased survival to 68% with alpha-interferon treatment [5,9,23]. Extra skeletal manifestations affecting the orbit, heart, and central nervous system (CNS) are associated with a poorer prognosis [24-26]. Constitutional symptoms such as fever, weight loss and weakness are frequent presenting observations. Diabetes insipidus in the second most common presenting feature and may precede the bone manifestations by several years [18]. Retroperitoneal, cardiac, and pulmonary involvement leading to chronic renal failure, cardiomyopathy, and severe interstitial lung disease, respectively, account for the majority of morbidity and mortality in patients with ECD [8,15].

Bone involvement is nearly a constant in ECD, characteristically affecting the appendicular skeleton. Typically, it involves the lower extremities more frequently and severely than the upper extremities [3]. The radiographic feature of symmetric diaphyseal and metaphyseal osteosclerosis is nearly pathognomonic, characterized by either diffuse or patchy increased density, coarsened trabeculae, and pronounced periosteal and endosteal cortical thickening resulting in the loss of the corticomedullary differentiation [3,5-7,27-29]. Lytic lesions are reported in 5% to 8% of cases [5].

ECD has a characteristic appearance on ^{99}Technetium bone scintigraphy with abnormally increased uptake in the meta-diaphyseal regions of the long bones [11,13]. MR imaging is particularly sensitive to changes in the bone marrow. The appearance of histiocytic infiltrates of ECD have been reported as homogeneously low signal intensity on T1-weighted images, and heterogeneously mixed areas of increased and decreased signal intensity on fluid-sensitive sequences along the diaphysis and metaphysis [8,30-33]. Relative sparing of the epiphysis has been a frequent observation on radiographic evaluation but partial epiphyseal involvement occurs in 45% of patients undergoing MR imaging, either as a homogeneous infiltrate that spares the subchondral bone or as a heterogeneous infiltrate [3]. Mature periosteal reactive changes occur in two-thirds of cases and bone infarcts also are frequent associated findings. Lytic lesions, while controversial, have been reported to occur in 33% of cases [33-35].

Derangement of the chemokine and cytokine networks is one of the underlying pathophysiology of ECD, and it is likely that our patient's initial inflammatory response may have been triggered by a common stimulus, such as the upper respiratory illness or the administration of a cephalosporin medication [36]. Severe hypercalcemia also has not been reported in patients with ECD. Lyders et al. reported a case of a 27-year-old woman who presented to the emergency room after having a seizure [35]. She had a 6-year history of seizures and biopsy-proven xantho-granulomatous infiltration of the brain. The serum calcium level was not reported in that patient. However, a pelvis CT showed lytic lesions in the iliac bones bilaterally and a bone survey showed diffuse osteopenia, compression fractures of the thoracic spine, and a left femoral neck fracture, features that are not characteristic of ECD. Our patient showed areas of lysis in both femora, the left ilium and in one lumbar vertebral body in addition to diffuse intense periostitis in the shafts of both fe-

mora. Many of these abnormalities were FDG-avid and evident on the initial FDG PET-CT scan. These were likely manifestations of acute osteolysis that eventually overwhelmed the calcium-phosphorus balance. Upon treatment of the hypercalcemic episode, his hospital course was largely self-limited. His symptoms had abated to the point that definitive treatment of his ECD was no longer required since it could have worsened his sinus infection. The follow-up FDG PET/CT scan performed 12 weeks after his hospital discharge showed decreased FDG-avid areas in the bone marrow and that the several of the lytic lesions had been replaced by diffuse sclerotic bone.

Although the diagnosis of ECD was made on the most recent hospital admission, two observations suggested that the disease in our patient may have been chronic. Periodontal disease has been reported in patients with ECD as a consequence of premature alveolar bone loss [37], which was noted on our patient's admission physical examination. In fact, after his discharged from the hospital, 17 of his teeth were extracted. The second observation was the presence of bone infarcts in his femur, which either occurs from either vascular obstruction secondary to periadventitial infiltration or intramedullary coagulative type of necrosis secondary to xantho-granulomatous cellular infiltration [38,39].

Currently, the first-line therapy for treatment of ECD is IFN-α and pegylated IFN-α (PEG-IFN-α) (Grade C2) [1,26,40,41]. Other treatment alternatives include imatinib mesylate [42], recombinant human interleukin-I receptor [43], cladribine [44,45], BRAF V600E kinase inhibitors vemurafenib and cobimetinib [46-49], MEK inhibitors cobimetinib and trametinib [46,49], and biologics anakinra, infliximab, and tocilizumab [45,50].

In summary, this case report illustrated a unique self-limited inflammatory ECD response triggered by an infection or cephalosporin allergy, eventually resulting in severe hypercalcemia. ^{18}F-FDG PET-CT imaging correlated closely to the patient's symptoms, as did the follow-up study. Once the calcium levels returned to normal, our patient did not require definitive immunosuppressive or disease-modifying therapy.

References

1. Diamond EL, Dagna L, Hyman DM, et al. Consensus guidelines for the diagnosis and clinical management of Erdheim-Chester disease. Blood. 2014;124:483-92.

2. Alexiou J, Klastersky J. Erdheim-Chester disease: a case report. Am J Case Rep. 2015;16:361-6.

3. Dion E, Graef C, Miquel A, et al. Bone involvement in Erdheim-Chester disease: imaging findings including periostitis and partial epiphyseal involvement. Radiology. 2006;238:632-9.

4. Diamond EL, Reiner AS, Buthorn JJ, et al. A scale for patient reported symptom assessment for patients with Erdheim-Chester disease. Blood Adv. 2019;3:934-8.

5. Veyssier-Belot C, Cacoub P, Caparros-Lefebvre D, et al. Erdheim-Chester disease: clinical and radiologic characteristics of 59 cases. Medicine. 1996;75:157-69.

6. Resnick D, Greenway G, Genant H, et al. Erdheim-Chester disease. Radiology. 1982;142:289-95.

7. Bancroft LW, Berquist TH. Erdheim-Chester disease: radiographic findings in five patients. Skeletal Radiol. 1998;27:127-32.

8. Gottlieb R, Chen A. MR findings of Erdheim-

Chester disease. J Comput Assist Tomogr. 2002;26:257-61.

9. Mamlouk MD, Aboian MS, Glastonbury CM. Case 245: Erdheim-Chester disease. Radiology. 2017;284:910-7.

10. Kirchner J, Hatzoglou V, Buthorn JB, et al. 18F-FDG PET/CT versus anatomic imaging for evaluating disease extent and clinical trial eligibility in Erdheim-Chester disease: results from 50 patients in a registry study. Eur J Nucl Med Mol Imaging. 2020; 1154-65.

11. Garcia-Gomez FJ, Acevedo-Banez I, Martinez-Castillo R, et al. The role of 18FDG, 18FDOPA PET/CT and 99mTc bone scintigraphy imaging in Erdheim-Chester disease. Eur J Radiol. 2015;84:1586-92.

12. Arnaud L, Malek Z, Archambaud F, et al. 18F-fluorodeoxyglucose-positron emission tomography scanning is more useful in follow-up than in the initial assessment of patients with Erdheim-Chester disease. Arthritis Rheum. 2009;60:3128-38.

13. Namwongprom S, Nunez r, Kim EE, et al. Tc-99m MDP bone scintigraphy and positron emission tomography/computed tomography (PET/CT) imaging in Erdheim-Chester disease. Clin Nucl Med. 2007;32:35-8.

14. Lin E. FDG PET/CT for biopsy guidance in Erdheim-Chester disease. Clin Nucl Med 2007;32:860-1.

15. Stenova E, Steno B, Povinec P, et al. FDG-PET in the Erdheim-Chester disease: its diagnostic and follow-up role. Rheumatol Int. 2012;32:675-8.

16. Young JR, Johnson GB, Murphy RC, et al. 18F-FDG PET/CT in Erdheim-Chester disease: imaging findings and potential BRAF mutation biomarker. J Nucl Med. 2018;59:774-9.

17. Haroche J, Charlotte F, Arnaud L, et al. High prevalence of BRAF V600E mutations in Erdheim-Chester disease but not in other non-Langerhans cell histiocytoses. Blood. 2012;120:2700-3.

18. Wilejto M, Abla O. Langerhans cell histiocytosis and Erdheim-Chester disease. Curr Opin Rheumatol 2012;24:90-6.

19. Dickson BC, Pethe V, Chung CT, et al. Systemic Erdheim-Chester disease. Virchows Arch. 2008;452:221-7.

20. Zaveri J, La Q, Yarmish G, et al. More than just Langerhans cell histiocytosis: a radiologic review of histiocytic disorders. Radiographics 2014;34:2008-24.

21. Haroche J, Arnaud L, Amoura Z. Erdheim-Chester disease. Curr Opin Rheumatol 2012;24:53-9.

22. Arnaud L, Hervier B, Neel A, et al. CNS involvement and treatment with interferon-alpha are independent prognostic factors in Erdheim-Chester disease: a multicenter survival analysis of 53 patients. Blood. 2011;117:2778-82.

23. De Filippo M, Ingegnoli A, Carloni A, et al. Erdheim-Chester disease: clinical and radiological findings. Radiol Med 2009;114:1319-29.

24. Arnoud L, Bach G, Zeitoun D, et al. Whole-body MRI in Erdheim-Chester disease. Rheumatology. 2012;51:948-50.

25. Haroche J, Amoura Z, Dion E, et al. Cardiovascular involvement, an overlooked feature of Erdheim-Chester disease: report of 6 new cases and a literature review. Medicine. 2004;83:371-92.

26. Hervier B, Arnaud L, Charlotte F, et al.

Treatment of Erdheim-Chester disease with long-term high-dose interferon-a. Semin Arthritis Rheum. 2012;41:907-13.

27. Evans S, Williams F. Case report: Erdheim-Chester disease: polyostotic sclerosing histiocytosis. Clin Radiol 1986;37:93-6.

28. Kenn W, Eck M, Allolio B, et al. Erdheim-Chester disease: evidence for a disease entity different from Langerhans cell histiocytosis? Three cases with detailed radiological and immunohistochemical analysis. Hum Pathol 2000;31:734-9.

29. Murray D, Marshall M, England E, et al. Erdheim-chester disease. Clin Radiol. 2001;56:481-4.

30. Kushihashi T, Munechika H, Sekimizu M, et al. Erdheim-Chester disease involving bilateral lower extremities: MR features. AJR Am J Roetngenol. 2000;174:875-6.

31. Bruil V, Brocq O, Pellegrino C, et al. Erdheim-Chester disease: typical radiological bone features for a rare xanthogranulomatosis. Ann Rheum dis. 2002;61:199-200.

32. Omos JM, Canga A, Velero C, et al. Imaging of Erdheim-Chester disease. J Bone Miner Res 2002;17:381-3.

33. Joo CU, Go YS, Kim IH, et al. Erdheim-Chester disease in a child with MR imaging showing regression of marrow changes. Skeletal Radiol 2005;34:299-302.

34. Egan AJ, Boardman LA, Tazelaar HD, et al. Erdheim-Chester disease: clinical, radiologic, and histopathologic findings in five patients with interstitial lung disease. Am J Surg Pathol. 1999;23:17-26.

35. Lyders EM, Kaushik S, Perez-Berenguer J, et al. Aggressive and atypical manifestations of Erdheim-Chester disease. Clin Rheumatol. 2003;22:464-6.

36. Arnaud L, Gorochov G, Charlotte F, et al. Systemic perturbation of cytokine and chemokine networks in Erdheim-Chester disease: a single-center series of 37 patients. Blood. 2011;117:2783-90.

37. Valdez IH, Katz RW, Travis WD. Premature alveolar bone loss in Erdheim-Chester disease. Oral Surg Oral Med Oral Pathol. 1990;70:294-6.

38. Serratrice J, Granel B, De Roux C, et al. "Coated aorta": a new sign of Erdheim-Chester disease. J Rheumatol. 2000;27:1550-3.

39. Brower AC, Worsham GF, Dudley AH. Erdheim-Chester disease: a distinct lipoidosis or part of the spectrum of histiocytosis. Radiology. 1984;151:35-8.

40. Braiteh F, Boxrud C, Esmaeli B, et al. Successful treatment of Erdheim-Chester disease, a non-Langerhans-cell histiocytosis, with interferon-alpha. Blood. 2005;106:2992-4.

41. Iaremenko O, Petelytska L, Dyadyk O, et al. Clinical presentation, imaging and response to interferon-alpha therapy in Erdheim-Chester disease: case-based review. Rheumatol Int. 2020;40:1529-36.

42. Janku F, Amin HM, Yang D, et al. Response of histiocytoses to imatinib mesylate: fire to ashes. J Clin Oncol. 2010;28:e633-6.

43. Aouba A, Geogin-Lavialle S, Pagnoux C, et al. Rationale and efficacy of interleukin-1 targeting in Erdheim-Chester disease. Blood 2010;116:4070-6.

44. Myra C, Sloper L, Tighe PJ, et al. Treatment of Erdheim-Chester disease with cladribine: a rational approach. Br J Ophthalmol.

2004;88:844-7.

45. Goyal G, Shah MV, Call TG, et al. Efficacy of biological agents in the treatment of Erdheim-Chester disease. Br J Haematol. 2018;183:520-4.

46. Diamond EL, Subbiah V, Lockhart AC, et al. Vemurafenib for BRAF V600-Mutant Erdheim-Chester disease and Langerhans cell histiocytosis: analysis of data from the histology-independent, phase 2, open-label VE-BASKET Study. JAMA Oncol. 2018;4:384-8.

47. Borys D, Nystrom L, Song A, et al. Erdheim-Chester disease with appendicular skeletal, renal and pleural involvement responding to Zelboraf (BRAF inhibitor) treatment: case report. Skeletal Radiol. 2016;45:1397-402.

48. Cohen-Aubart F, Emile J-F, Carrat F, et al. Targeted therapies in 54 patients with Erdheim-Chester disease, including follow-up after interruption (the LOVE study). Blood. 130:1377-80.

49. Diamond EL, Durham BH, Ulaner GA, et al. Efficacy of MEK inhibition in patients with histiocytic neoplasms. Nature. 2019;567:521-4.

50. Cohen-Aubart F, Maksud P, Emile J-F, et al. Efficacy of infliximab in the treatment of Erdheim-Chester disease. Ann Rheum Dis. 2018;77:1387-90.